ADELE

Analyse et impact de Défauts Locaux de Cœur de pile sur le fonctionnement des stacks PEMFC

CONTEXT AND OBJECTIVES

Growing H_2 industry BUT still **limitations of PEMFC stacks and systems** due **to durability and expensive cost**

- **Membrane-Electrodes Assemblies (MEA):** key element for performance / durability **(50% of stack cost)**
- **Integration and assembly of very thin of components** (Membrane < 10 µm) and active layers thickness (~ few µm)
- Actors strive to **produce homogeneous MEAs and to develop/use suitable quality control to detect impactful defects (type & size)**

/!\ Additional cost due to scraps and possible durability issue caused by defects in MEA components or MEA assembly /!

→ **Evaluate the impact of realistic MEA defects** on the durability of a cell and **how a defective cell triggers degraded behaviours on neighbouring cells in stack**

→ **Establish the link between defect and degradation mechanisms** at stake and transposition to others types of MEAs: PEMWE, AEMWE…

→ **Determine the acceptable defect type/size *vs.* targeted lifetime**

80 kW PEMFC Stack | *Stack components: MEA & Bipolar plates* | *Real defect on commercial MEA*

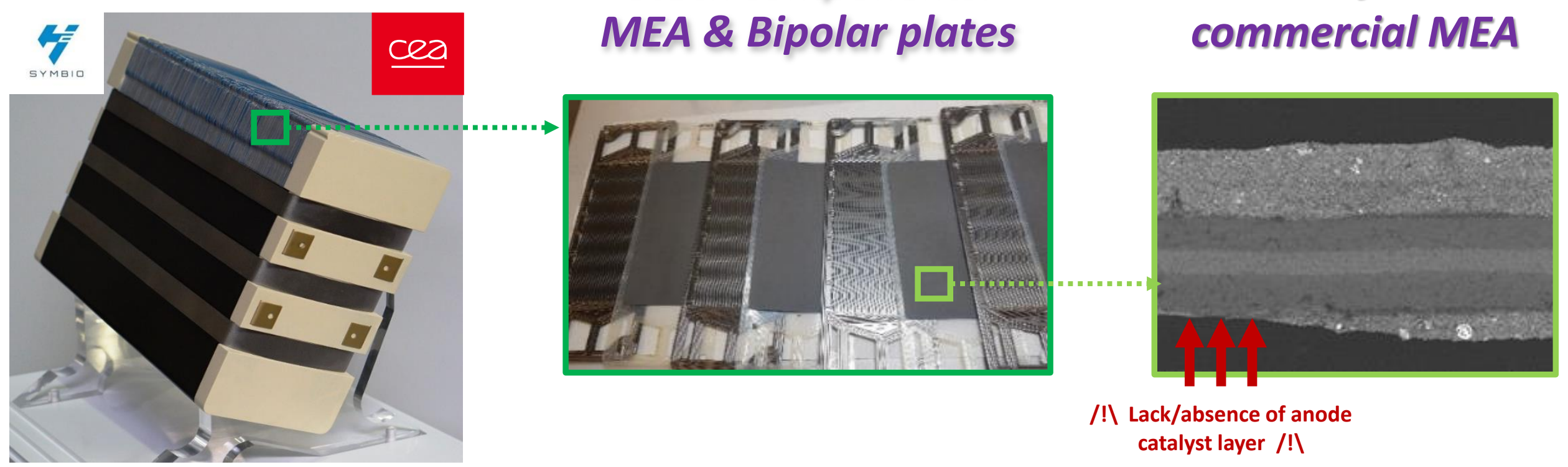

/!\ Lack/absence of anode catalyst layer /!\

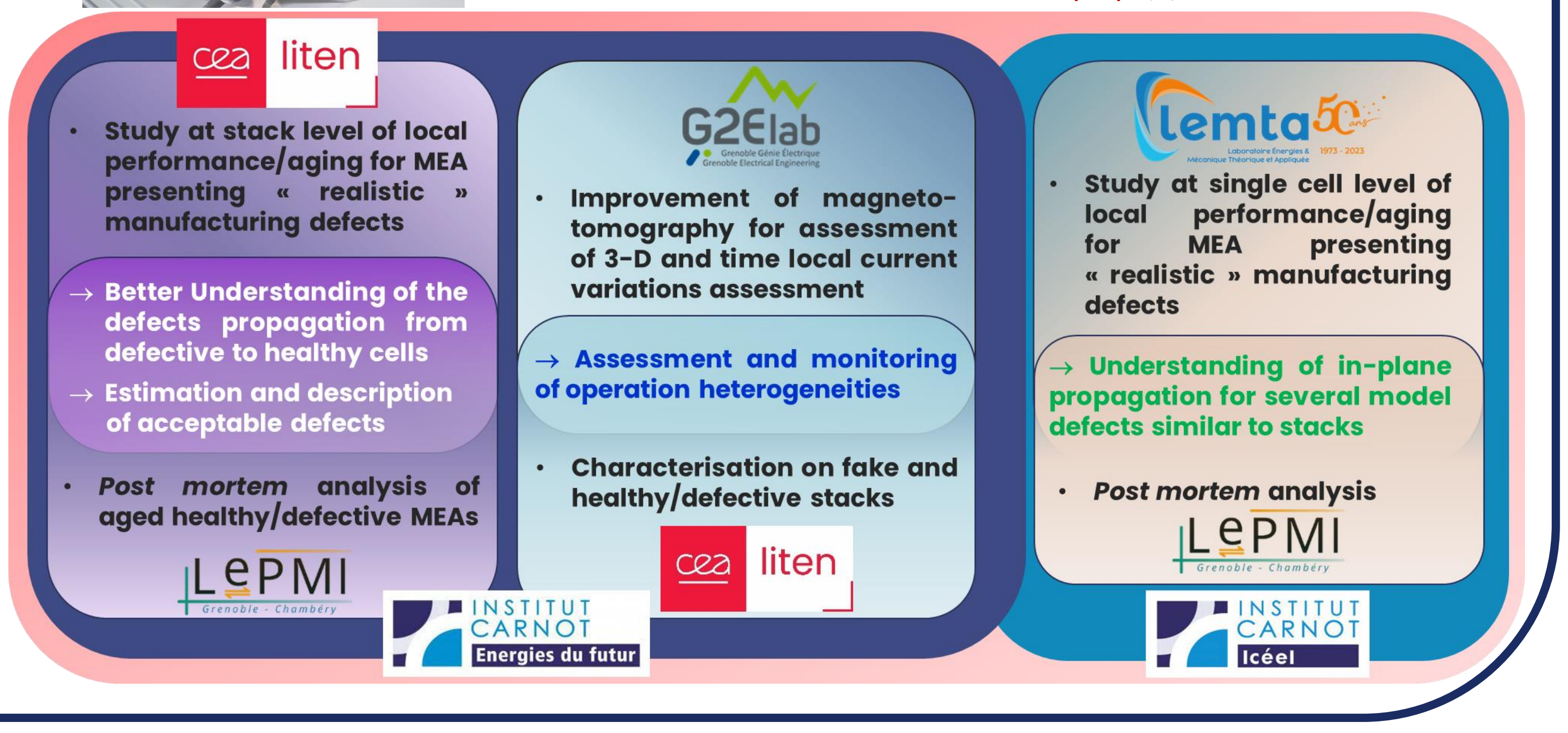

cea liten

- Study at stack level of local performance/aging for MEA presenting « realistic » manufacturing defects

→ Better Understanding of the defects propagation from defective to healthy cells

→ Estimation and description of acceptable defects

- *Post mortem* analysis of aged healthy/defective MEAs

G2Elab

- Improvement of magneto-tomography for assessment of 3-D and time local current variations assessment

→ Assessment and monitoring of operation heterogeneities

- Characterisation on fake and healthy/defective stacks

lemta

- Study at single cell level of local performance/aging for MEA presenting « realistic » manufacturing defects

→ Understanding of in-plane propagation for several model defects similar to stacks

- *Post mortem* analysis

EXPERIMENTAL APPROACH

Impact of defects

MEA production
Realistic defects

Defect ~2% active area

Stack Assembly

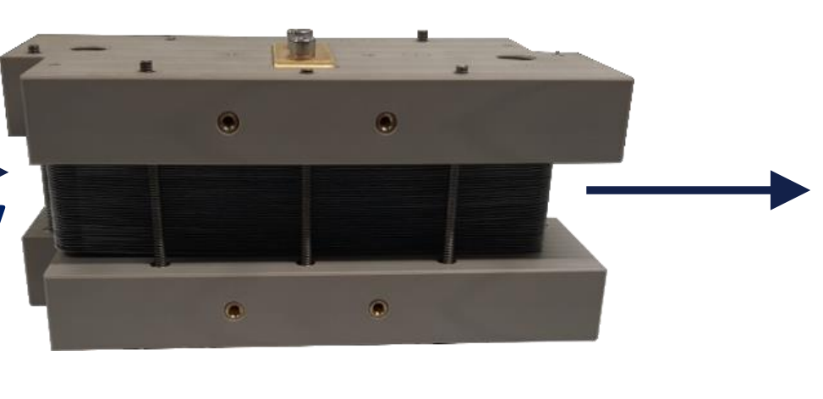

Mix of healthy and defective MEA

Quantification of degradation

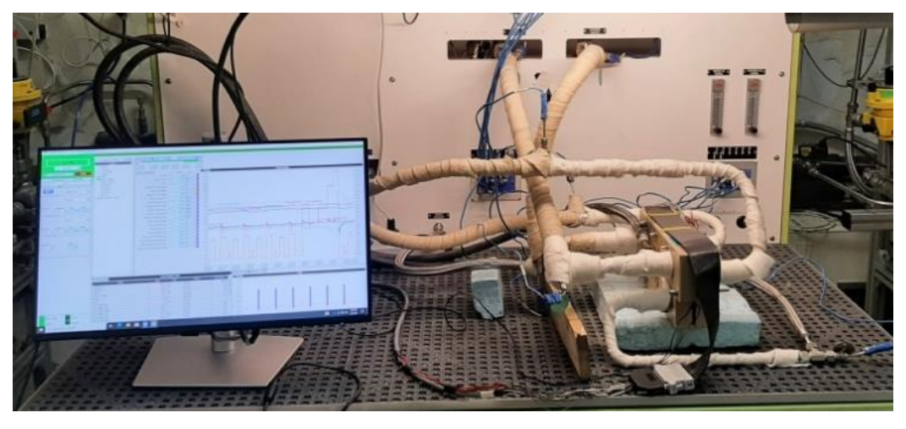

Performance and durability tests on lab bench

Influence of defects on stack lifetime

Detection

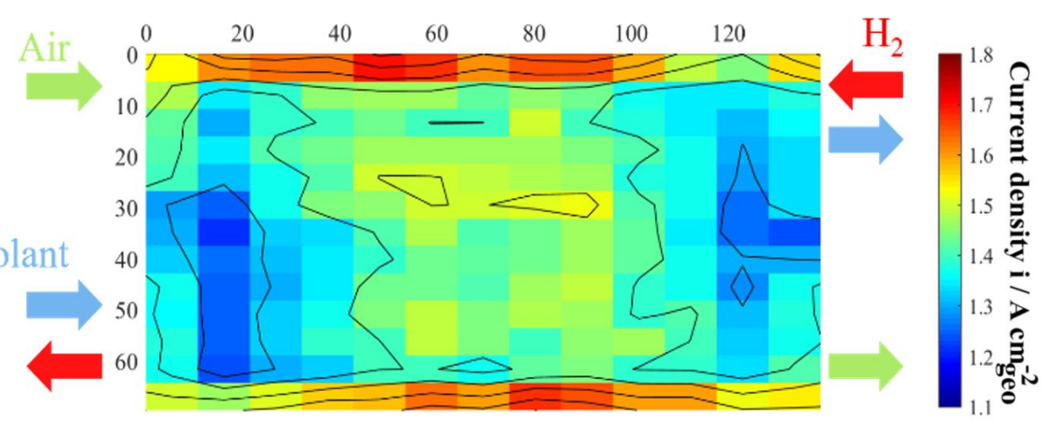

Improvement of local current measurements with S++® card (intrusive)

Detection

Design of new sensor frame around the stack

Measurements on fake and real stacks

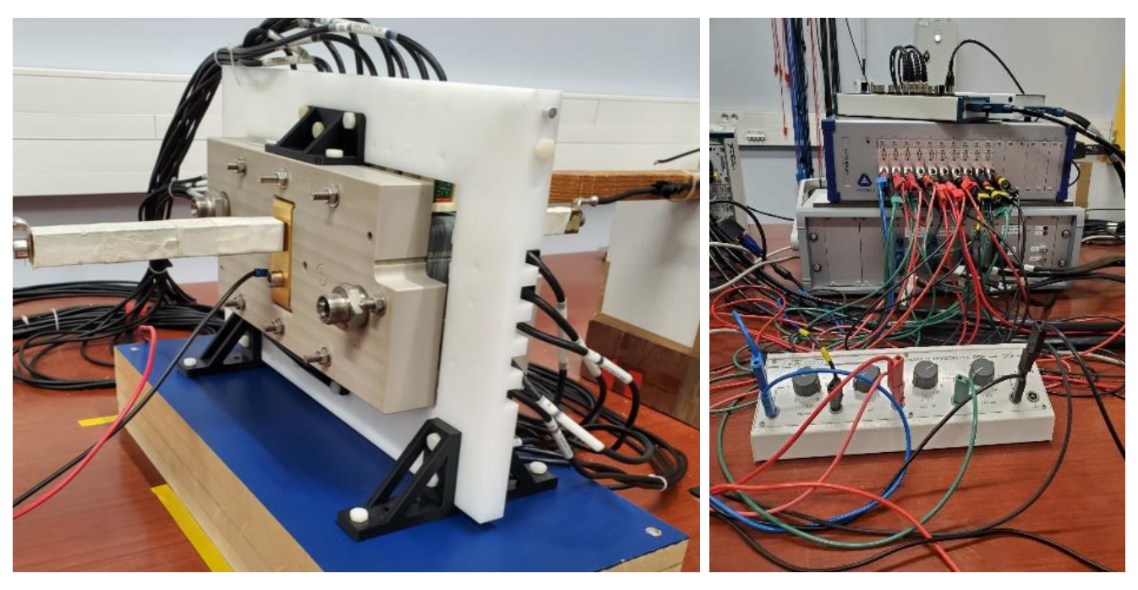

Improvement of magneto-tomographic tool (non-intrusive)

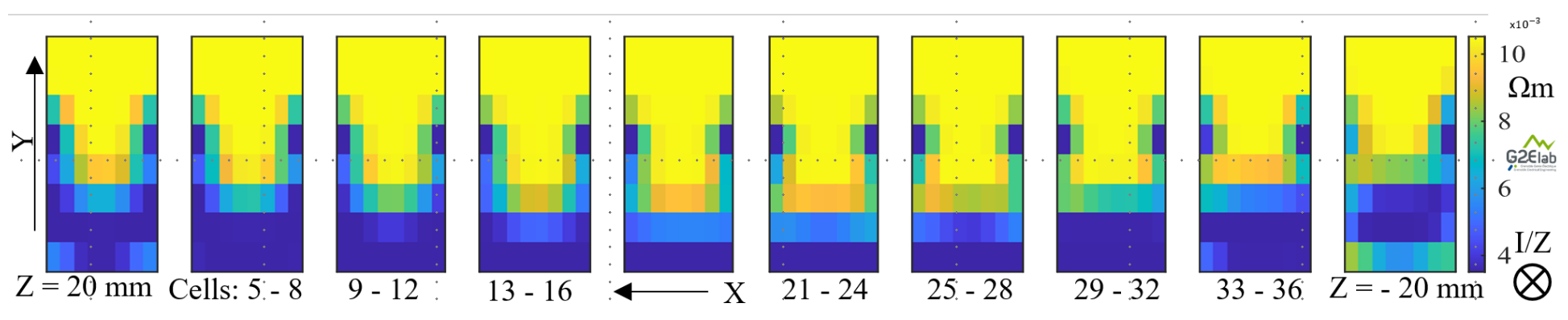

First results: effect of unbalanced compression on local resistivity distribution along a fake stack

CEA Stack design: 100 cm² active area
Stack size: 6 to 10 cells
MEA: SoA reference PEMFC95 *(ongoing PEPR-H2 project)*
Anode/Cathode: Pt/HSAC 0.1/0.3 mg_{Pt}/cm^2
Membrane: Gore M788.12
Gas Diffusion Layer (GDL) : H14C15 Freundenberg

Model defects considered:

- Lack of anode active layer (2 cm²) at anode inlet or outlet
- Absence of Microporous Layer on GDL (2 cm²)

Durability test

1,000 h FC-DLC dynamic operation (from NEDC driving cycle) with **periodic electrochemical characterisations** (polarisation curves, cyclic voltammetry (CV) and impedance)

MEA post-mortem analysis

- MEA observations by SEM / HRTEM
- Membrane structure evolution
- MEA sampling and testing in 2 cm² single cell

TOWARDS RELIABLE AND ADVANCED ELECTROCHEMICAL CHARACTERISATIONS IN STACKS

Global cell characterisations accessible by CV measurements

/!\ Limited connection on bipolar plates and/or full stack polarisation are often problematic (ohmic drop & collateral damage) /!

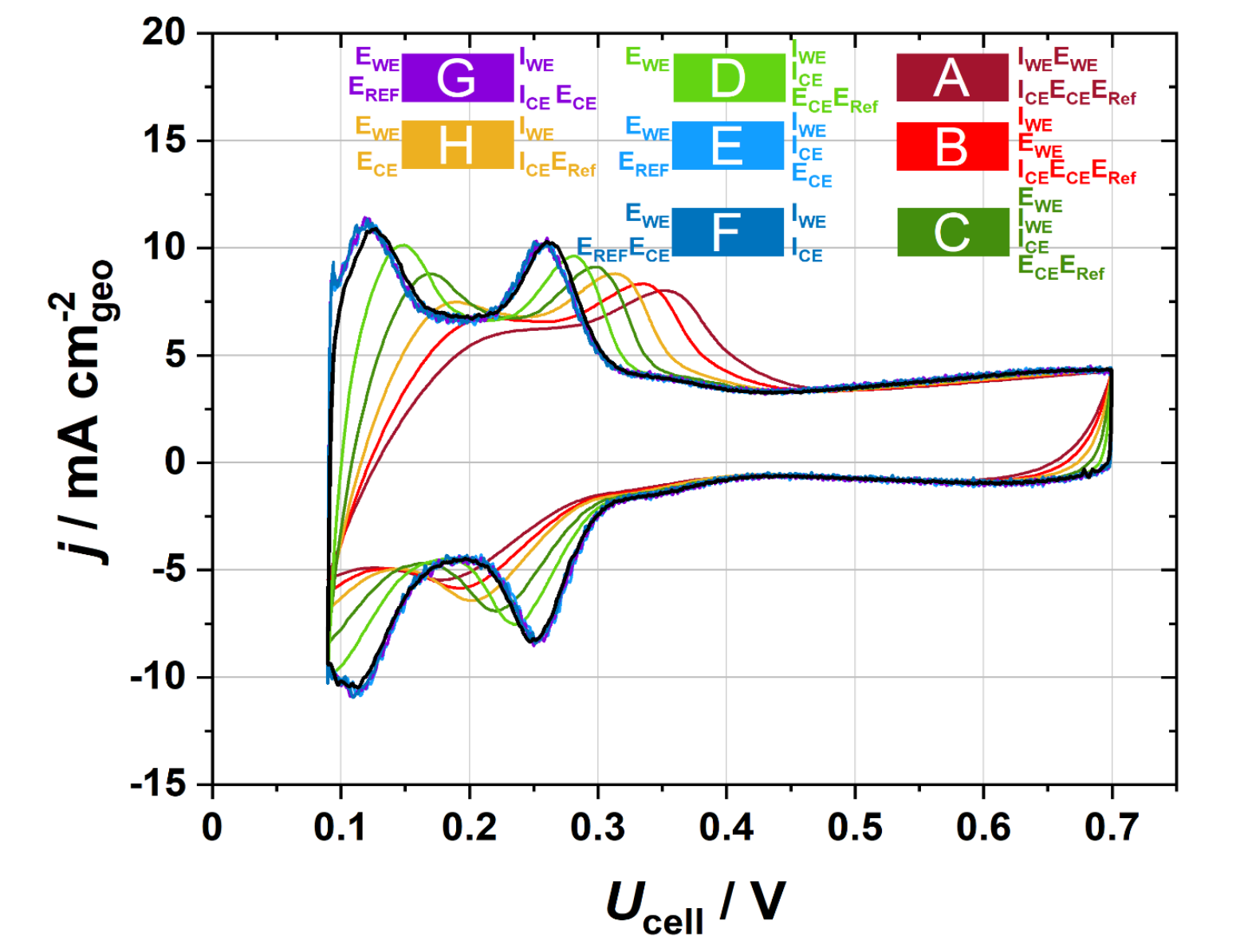

Global CV on individual cell in stack: impact of I & E connections on measurement quality

DOs and DON'Ts for CV on PEMFC STACK

- ✓ **Reliable and correct CV measurement possible** via **individual cell polarisation** in stacks with **proper connections (4 pins)**
- ✓ **No risk to damage other cells** (not polarised)
- ✓ **Conventional I & E range for potentiostat sufficient (independent of stack size)**
- ✓ **Close Ref & E_{WE} pins** if possible otherwise use dynamic ohmic drop correction

What about local cell characterisations by CV measurements ?

Local information on MEA properties during stack testing: needed to further understand the **impact of MEA defects** on **local operation** and **aging**
Can local CV be acquired during non-operating characterisation with $S^{++®}$ device for much smaller current (1 – 10 mA/cm²) ?

Local CV on healthy and homogenous MEA: impact of potentiostat connection on current distribution measured by S++®

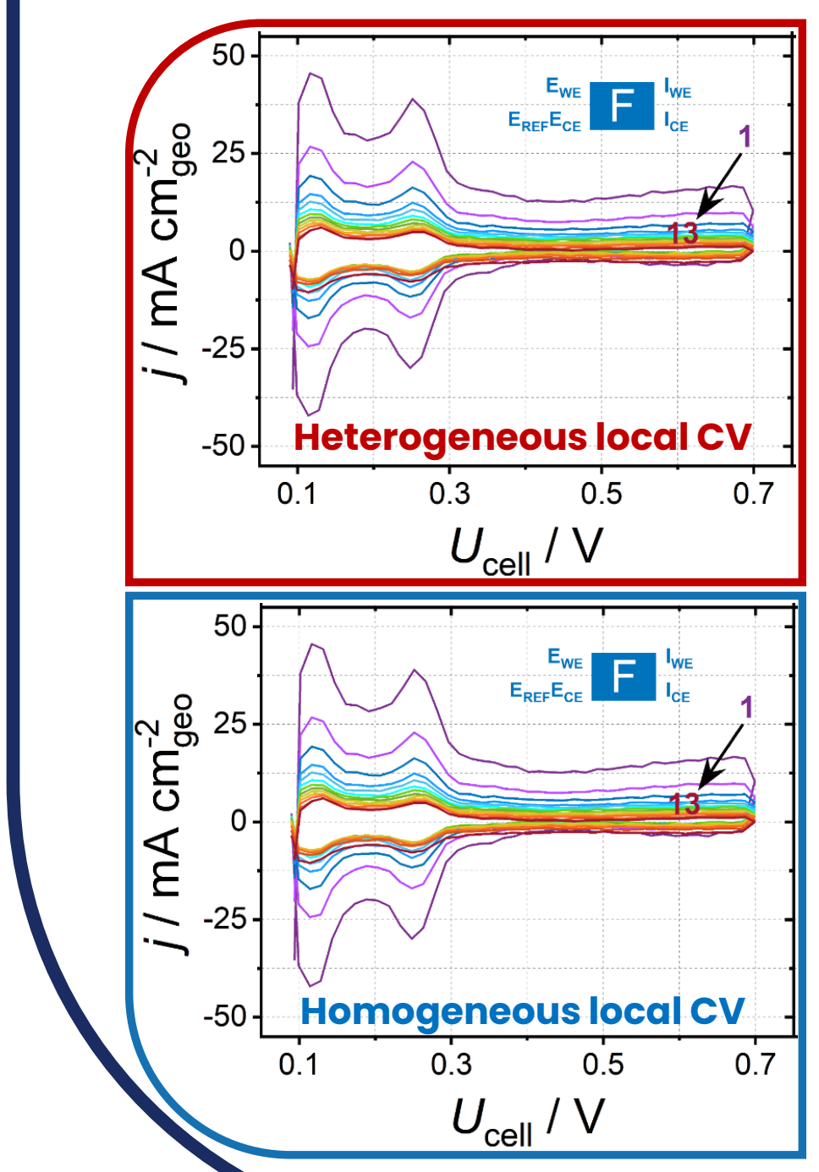

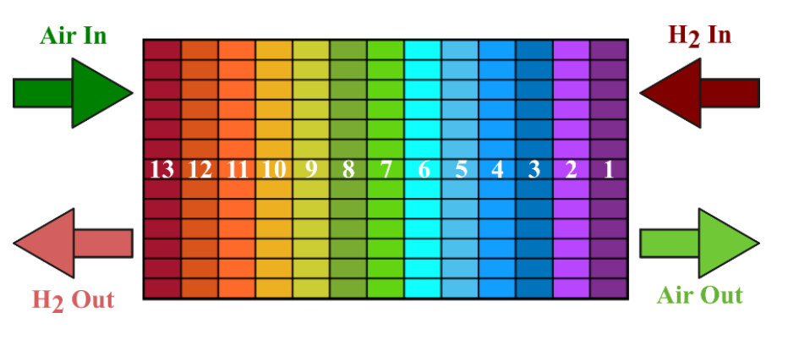

/!\ Bad connections' configurations can generate artefacts on local CV due to current redistribution in bipolar plates **/!**

Individual cell connection not suitable for local CV

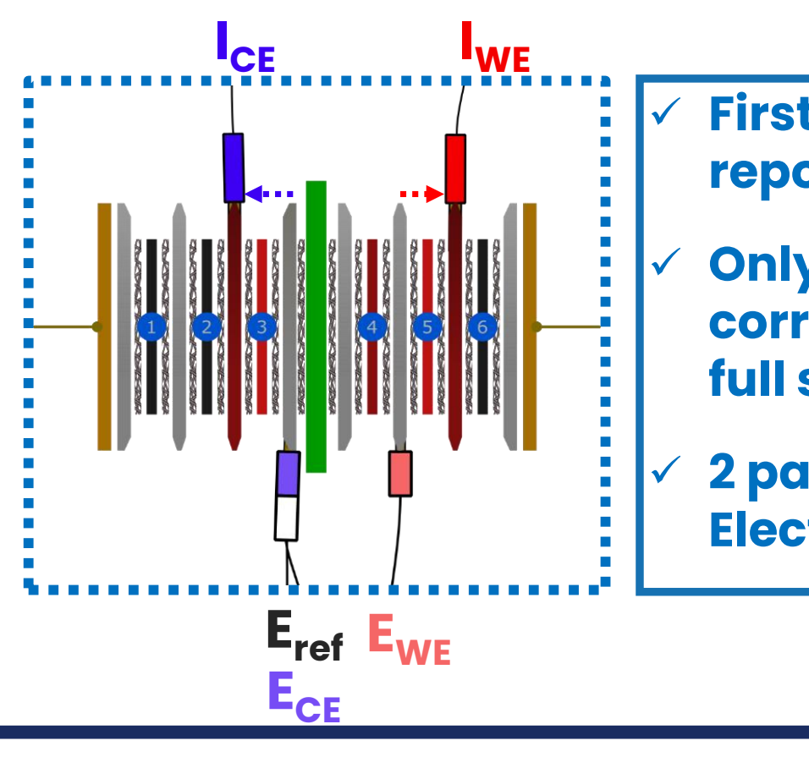

- ✓ **First time** that such **successful use of S++® is reported for local CV to our knowledge**
- ✓ **Only overlapped cells connections allow correct local CV measurements** and **avoid full stack polarisation** (only 3 cells polarised)
- ✓ **2 papers accepted in Journal of Applied Electrochemistry**

DURABILITY COMPARISON BETWEEN HEALTHY AND DEFECTIVE STACKS

Evolution of stack performance during FD-DLC tests

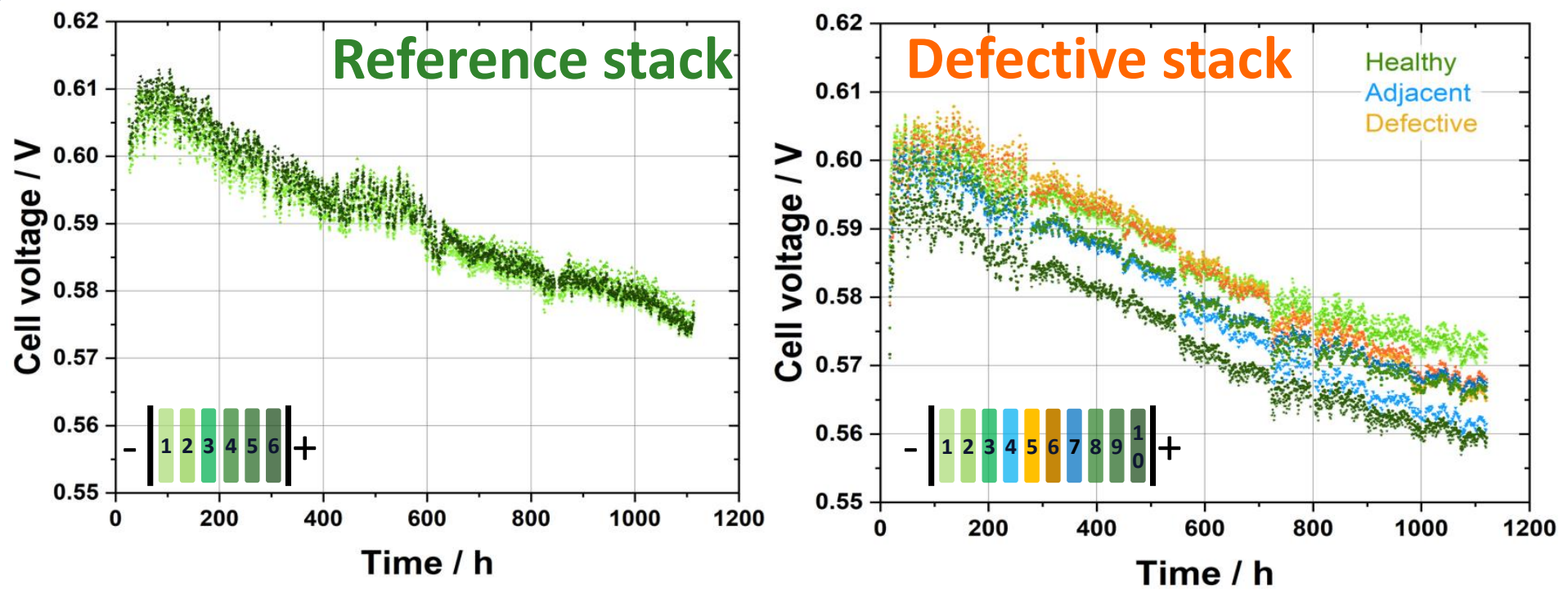

Cell voltage evolution during FC-DLC aging (1.25 A/cm²)

Defective stack *vs.* Reference:

- **Slightly lower global performance & higher dispersion** of cell voltages
- **Defective cells: better initial performance**
- **Adjacent** and **healthy MEAs placed after the defects** showed **degraded performance**

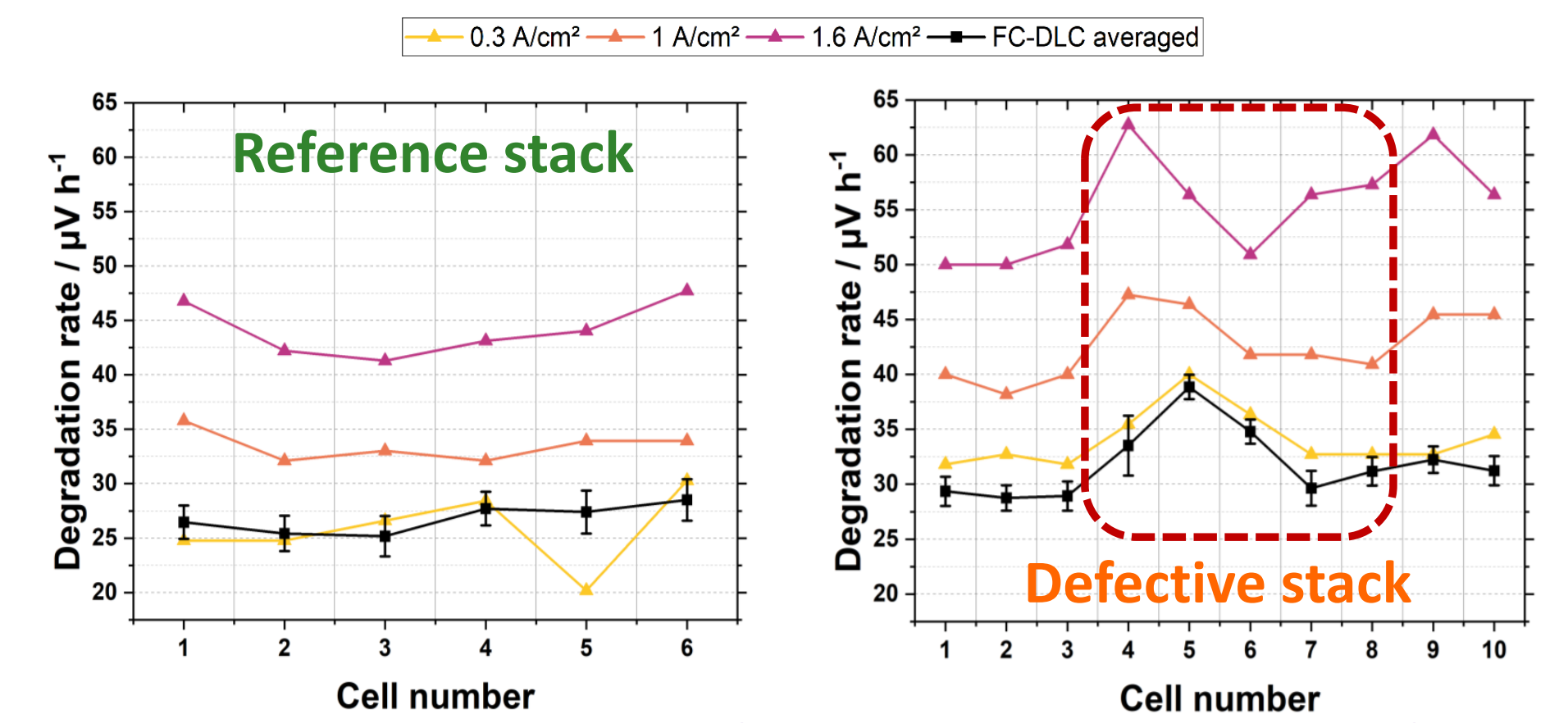

Individual degradation rate from polarisation curves after 1,100 h

- **Clear effect** of the presence of **defective MEA on degradation rate distribution** in the stack

→ **Slightly faster degradation rates**
→ **Higher degradation** of **defective** and **adjacent cells**
→ **Propagation of small-size defects**

MEA properties evolution during aging

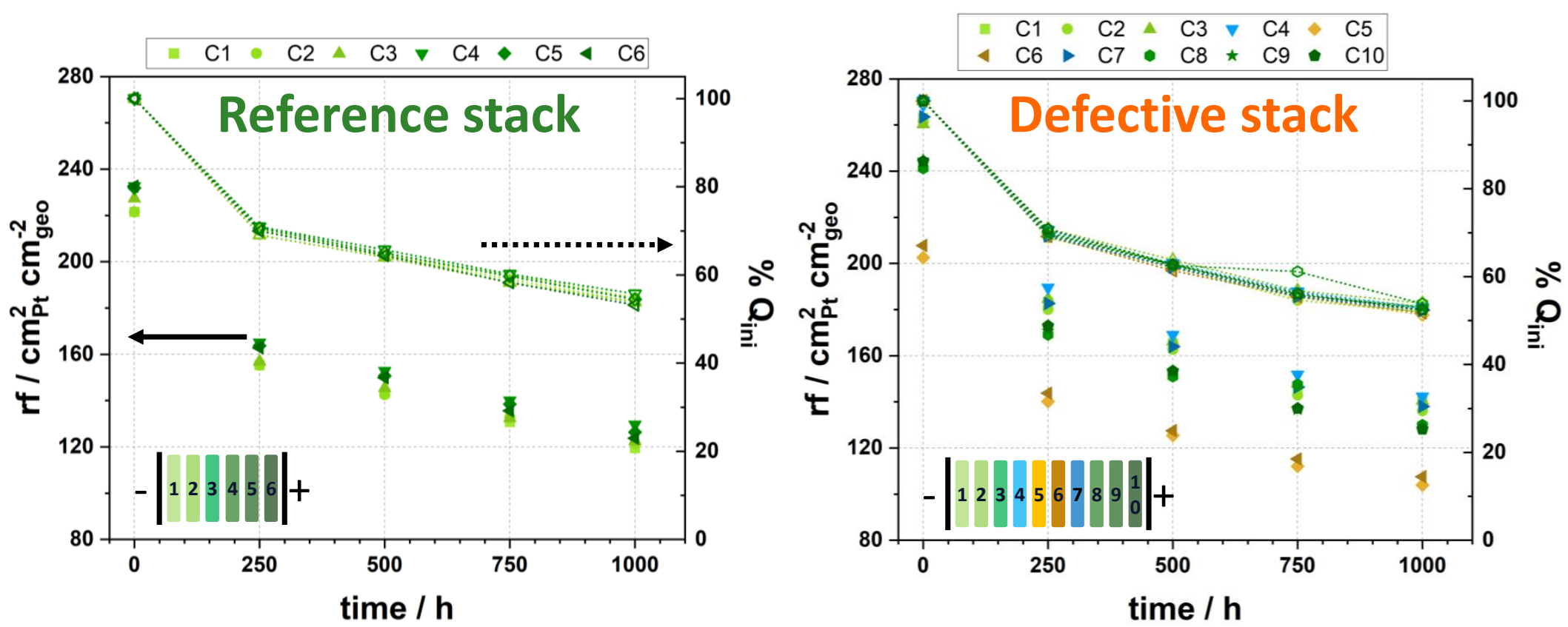

Evolution of cathode Pt active area during aging

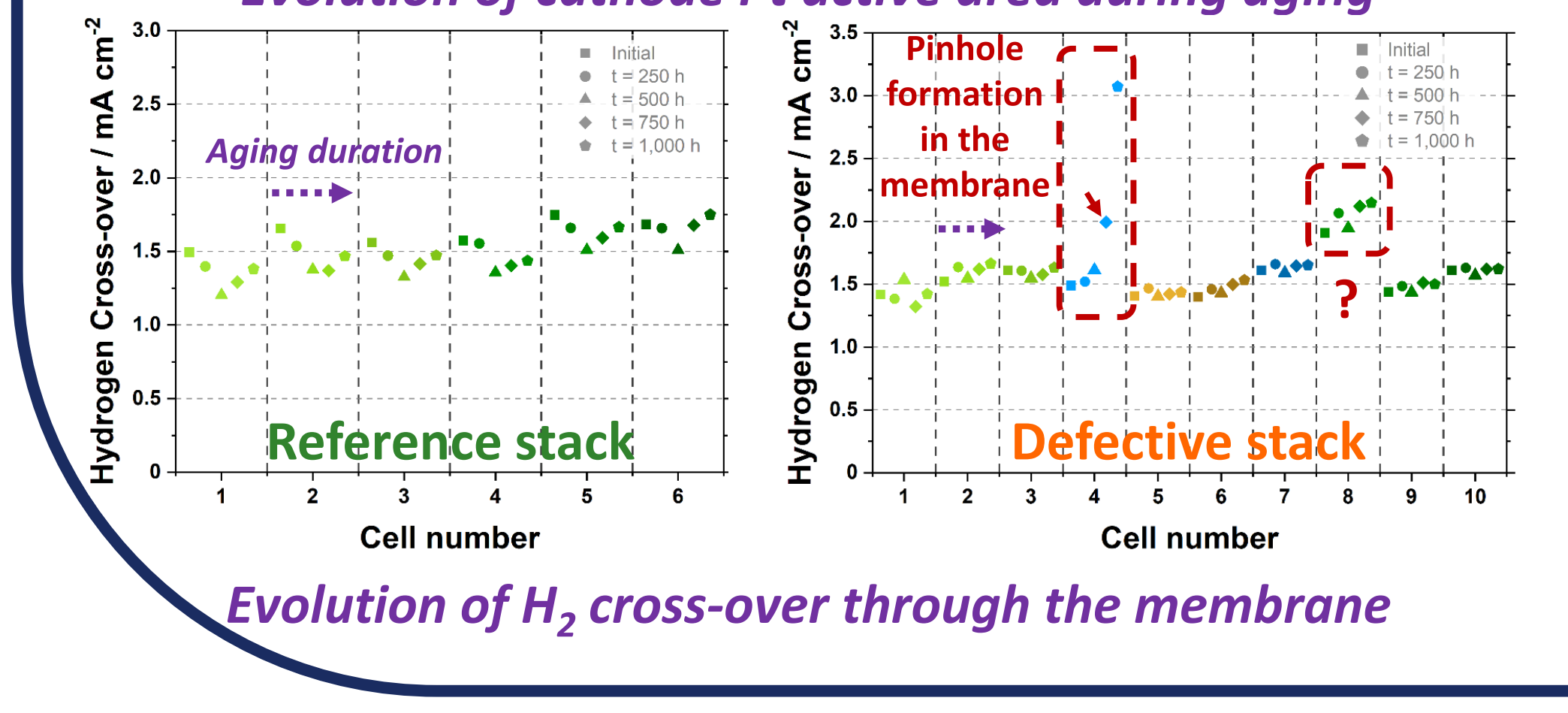

Evolution of H_2 cross-over through the membrane

- **Larger discrepancy in initial Pt active area for the defective stack among all cells: effect of the defects ?**
- **Similar relative active area losses during FC-DLC aging** between **reference** and **defective stacks**
- **No membrane physical degradation in reference stack**
- **Higher susceptibility of membrane weakening** on **adjacent cells**

→ Already observed in previous LOCALI ANR project with much larger defects

WHAT'S NEXT IN 2026 IN ADELE ?

→ **Local physical and electrochemical *post mortem* analysis on reference and 1st defective stack in progress**
→ **Two other types of MEA defects to be tested in short-stacks and then analysed**
→ **Comparison stack *vs.* small single cell testing and aging on similar defects**
→ **Magneto-tomography to be applied on PEMFC stack to detect defects during operation and monitor stack aging**

RIASSE Raphaël

MICOUD Fabrice

ROSINI Sébastien

09/12/2025

ADELE

Tomographie Magnétique de la Pile à Combustible à Hydrogène

Abstract

This article presents a new inverse algorithm based on magnetic tomography for fuel cell stack diagnostics. The aim is to determine the local internal resistivities of fuel cell stacks from external magnetic field measurements. The inverse problem is solved by minimizing the difference between the simulated magnetic field and the measured magnetic field. Sensitivities are calculated using the adjoint state method, and numerical results are presented shown on a 3D-fault.

Scope

Hydrogen Fuel Cell Stacks
as part of the Energy Transition

Hurdles such as:
Reduced **reliability** and **performance** losses
Caused by: Drying / Flooding
Fuel / oxidant starvation
Catalyst degradation
Catalyst distribution

Diagnostic Tools are needed which are:

1. Non-invasive
2. Able to localize faults

Magnetic tomography

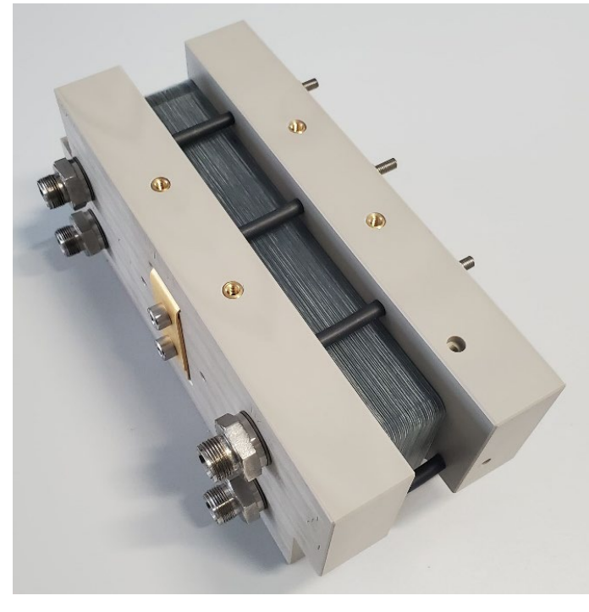

Magnetic Tomography

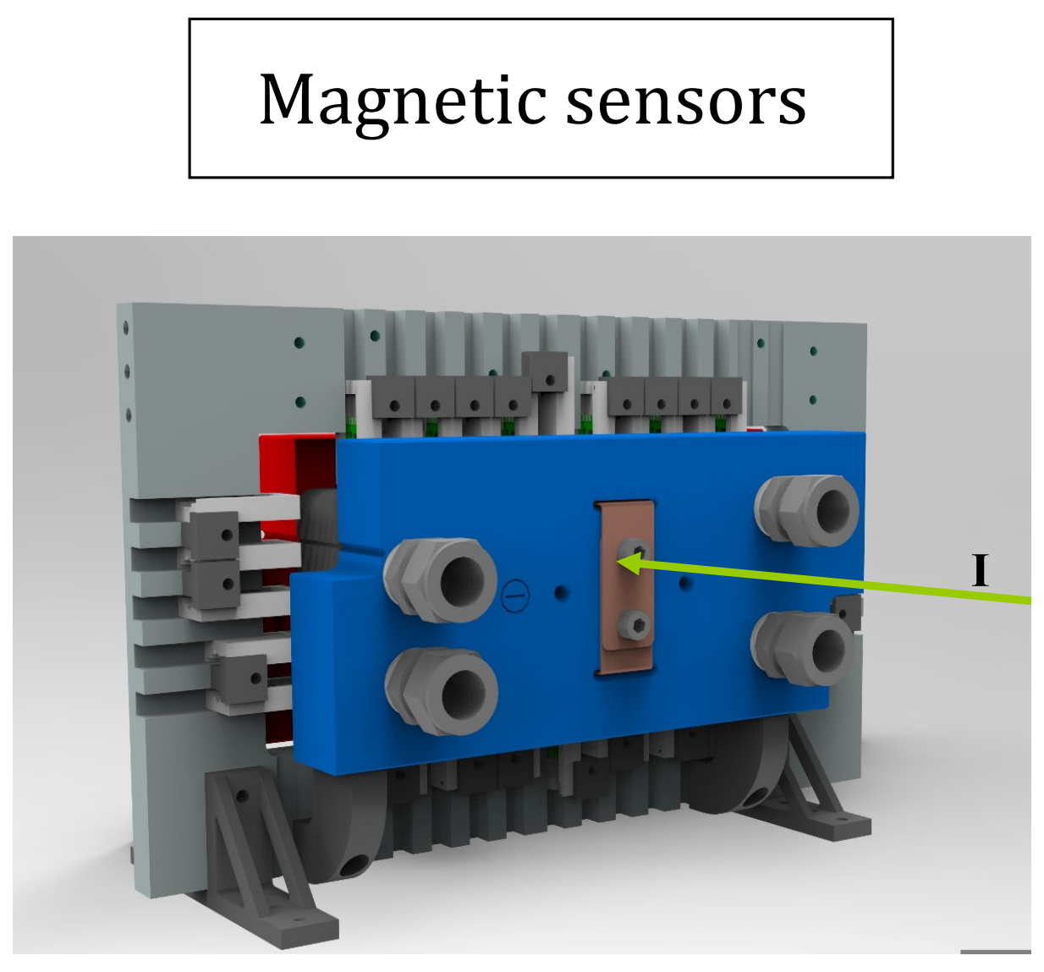

Inverse Problem Formulation

Find local fault by identifying local resistivities such that:

1. Measured Magnetic signature and of the Electrocinetic Model fit
2. Model voltage respects Measured Stack Voltage

Formulation of the inverse Problem as an optimization approach:

$$\widehat{\rho} = \underset{\rho}{\arg\min} \left(\|B_m - B_s(J(\rho))\|^2 + \alpha \|\mathbf{L}\rho\|^2 \right)$$

$$\text{s.t.} \quad U_s(\rho) - U_m = 0 \quad \text{(Nonlinear Constraint)},$$

$$\rho_{min} \leq \rho \leq \rho_{max} \ \text{(Bounds)}.$$

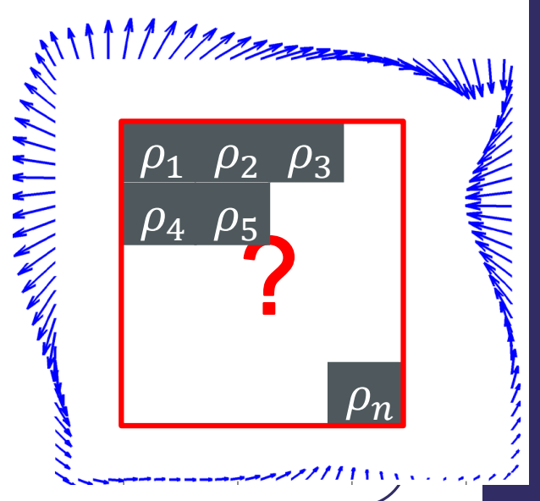

Challenge:

Compute derivative of cost function and constraints satisfying Electrokinetic equations with imposed current (FEM-Model)

Inverse Method by non-linear Optimization

1. FEM-Modelling at Constant J

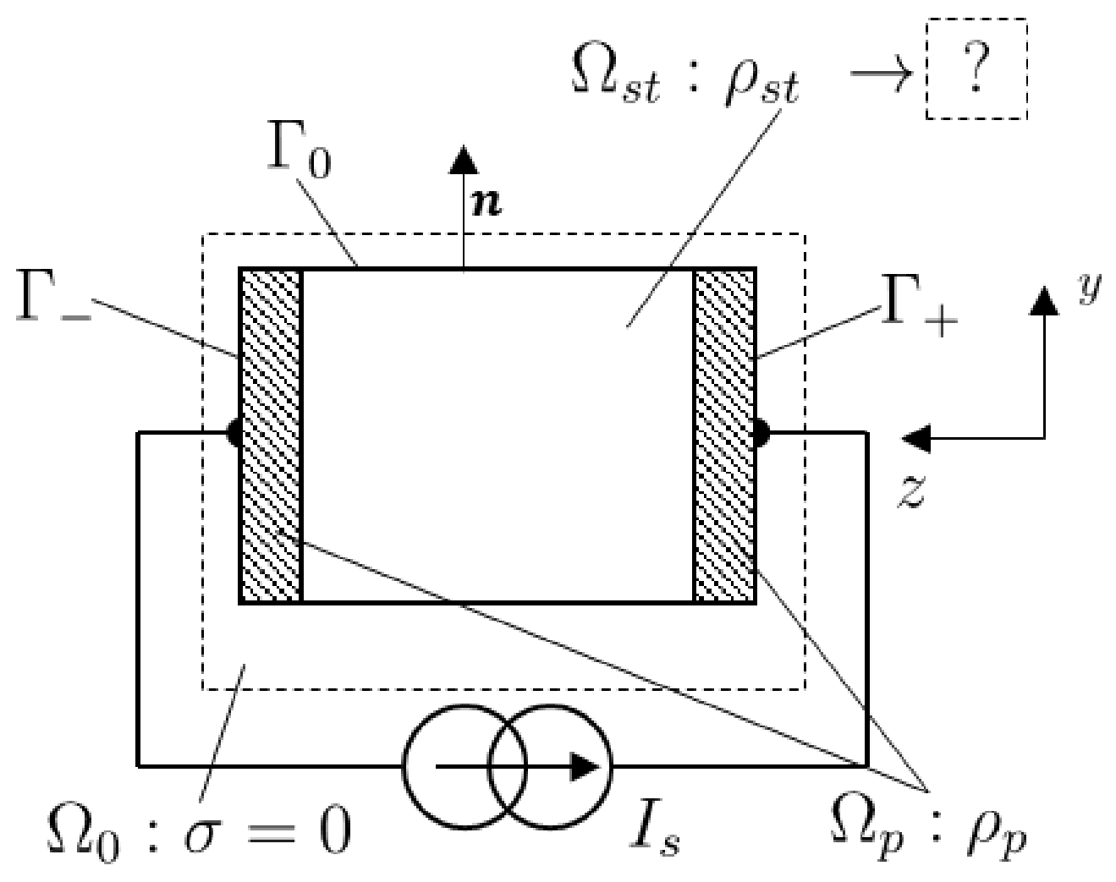

- Electrokinetic equations: $E = -\nabla U \quad E = \rho \cdot J \quad \nabla \cdot J = 0$
- Boundary conditions: $\Gamma_- : \int J_n = -I_s \ \ \Gamma_+ : \int J_n = I_s \ \ \Gamma_0 : \int J_n = 0$
- J interpolation on face shape functions (Whitney 2-form) $J = \sum_j \omega_j I_j$

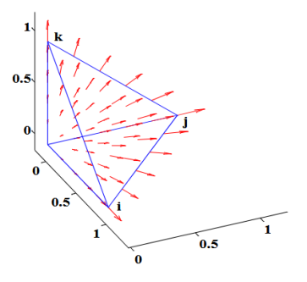

- Galerkin projection on test shape function: $\int_\Omega \omega_i \cdot \rho \cdot J \, \mathrm{d}\Omega = -\int_\Omega \omega_i \nabla U \, \mathrm{d}\Omega$
- Integration of Impedance matrix system

$$\mathbf{R}I = U \qquad U_i = -\int_\Omega \omega_i \nabla U \, \mathrm{d}\Omega \qquad \mathbf{R}_{i,j} = \int_\Omega \omega_i \omega_j \rho \, \mathrm{d}\Omega$$

- Free divergence of J obtained with incidence matrix $\mathbf{M_s}$ and $\mathbf{M_R}$:

$$\underbrace{\begin{bmatrix} \mathbf{M_S R M_R}^T & \mathbf{M_S} \\ \mathbf{M_S}^T & \mathbf{0} \end{bmatrix}}_{\mathbf{K}} \underbrace{\begin{bmatrix} I_{\text{loop}} \\ U_S \end{bmatrix}}_{x} = \underbrace{\begin{bmatrix} 0 \\ I_S \end{bmatrix}}_{S_H}$$

- Computation of B with integration of Biot-Savart law $B = \frac{\mu_0}{4\pi} \int_\Omega J(\rho) \times \frac{r}{|r|^3} \mathrm{d}\Omega \Rightarrow B_s = \mathbf{A} \ J(\rho)$

2. Compute Sensitivities with **Adjoint Method**[2]

1. Objective Function:

$$r(J(\rho)) = ||B_m - \mathbf{A}J(\rho)||^2$$

$$\frac{\mathrm{d}}{\mathrm{d}\rho}(r(J(\rho))) = \cancel{\frac{\partial r}{\partial \rho}}^{=0} + \frac{\partial r}{\partial J^{\mathrm{T}}} \frac{\partial J}{\partial \rho} \Rightarrow \frac{\mathrm{d}r(\rho)}{\mathrm{d}\rho} = \frac{\partial r}{\partial x^{\mathrm{T}}} \frac{\partial x}{\partial \rho}$$

Step 1:

$$\underbrace{\begin{bmatrix} \mathbf{M_R R}(\rho)\mathbf{M_R}^{\mathrm{T}} & \mathbf{M_S} \\ \mathbf{M_S}^{\mathrm{T}} & \mathbf{0} \end{bmatrix}}_{\mathbf{K}} \underbrace{\begin{bmatrix} \frac{\mathrm{d}I_{\text{loop}}}{\mathrm{d}\rho} \\ \frac{\mathrm{d}U_S}{\mathrm{d}\rho} \end{bmatrix}}_{\frac{\mathrm{d}x}{\mathrm{d}\rho}} = - \underbrace{\begin{bmatrix} \mathbf{M_R}\frac{\mathrm{d}\mathbf{R}(\rho)}{\mathrm{d}\rho}\mathbf{M_R}^{\mathrm{T}} & \mathbf{0} \\ \mathbf{0} & \mathbf{0} \end{bmatrix}}_{-\frac{\mathrm{d}\mathbf{K}}{\mathrm{d}\rho}} \underbrace{\begin{bmatrix} I_{\text{loop}} \\ U_S \end{bmatrix}}_{x}$$

$$\frac{\mathrm{d}x}{\mathrm{d}\rho} = \boxed{-\mathbf{K}^{-1}} \frac{\mathrm{d}\mathbf{K}}{\mathrm{d}\rho} x$$

Costly!

Use Adjoint State Method

Step 2: $\mathbf{K}^{\mathrm{T}}\lambda = \frac{\mathrm{d}r}{\mathrm{d}x} \rightarrow \frac{\mathrm{d}x}{\mathrm{d}\rho} = -\mathbf{K}^{-1}\frac{\mathrm{d}\mathbf{K}}{\mathrm{d}\rho}x$ $\boxed{\frac{\mathrm{d}r(\rho)}{\mathrm{d}\rho} = -\lambda \frac{\mathrm{d}\mathbf{K}}{\mathrm{d}\rho}x}$

Step 3: $\frac{\partial}{\partial J}(r(J(\rho))) = 2(\mathbf{A}^{\mathrm{T}}\mathbf{A}J(\rho) - (B_m^{\mathrm{T}}\mathbf{A})^{\mathrm{T}})$

2. Constraint Function analog to objective function:

$$0 = U_s(\rho) - U_m$$

$$\frac{\mathrm{d}U_s(\rho)}{\mathrm{d}\rho} = \frac{\partial U_s}{\partial x^{\mathrm{T}}} \frac{\partial x}{\partial \rho}$$

Set adjoint state:

$$\mathbf{K}^{\mathrm{T}}\lambda_{U_s} = \frac{\partial U_s}{\partial x} = \begin{bmatrix} 0 \\ \vdots \\ 1 \end{bmatrix}$$

$$\boxed{\frac{\mathrm{d}U_s(\rho)}{\mathrm{d}\rho} = -\lambda_{U_s} \frac{\mathrm{d}\mathbf{K}}{\mathrm{d}\rho} x}$$

3. Regularization

Problem is ill-posed
→ Supposition of regular ρ in the beginning of the FC-Stack life
→ Add regularization term
→ Chose α with L-Curve method[4]

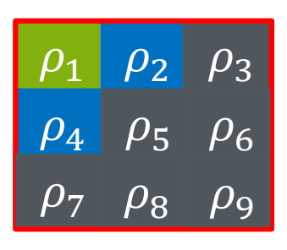

$$\mathbf{L} = \begin{bmatrix} 1 & -\frac{1}{2} & 0 & -\frac{1}{2} & 0 & \dots \\ & & & & & \dots \\ & & & & & \dots \end{bmatrix}$$

$$Y(\rho) = \alpha||\mathrm{L}\rho||^2$$

$$\frac{\partial Y(\rho)}{\partial \rho} = 2\alpha \mathrm{L}^{\mathrm{T}}\mathrm{L}\rho$$

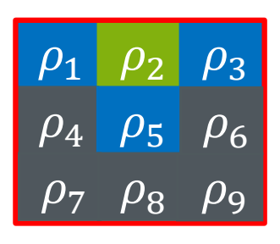

$$\mathbf{L} = \begin{bmatrix} 1 & -\frac{1}{2} & 0 & -\frac{1}{2} & 0 & \dots \\ -\frac{1}{3} & 1 & -\frac{1}{3} & 0 & -\frac{1}{3} & \dots \\ \dots & \dots & \dots & \dots & \dots & \dots \end{bmatrix}$$

4. Optimization Algorithm

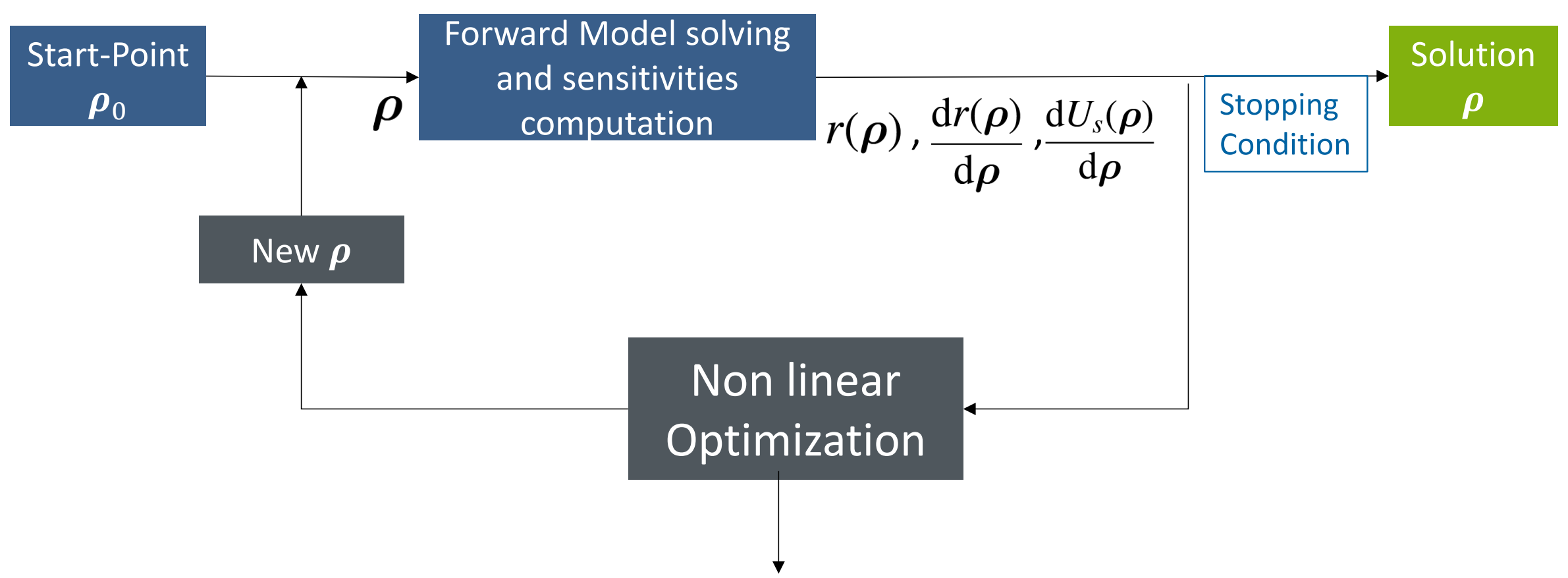

Interior Point Algorithm → Compose Lagrangian of function, constraints and bounds
Gradient Descend → minimize Lagrangian[2]
Broyden-Fletcher-Goldfarb-Shanno (BFGS) → Hessian approximation[3]

Results

Numerical Measurement

Procedure:

1. Solve Forward problem with a ρ
2. Add noise
3. Solve with inverse Method

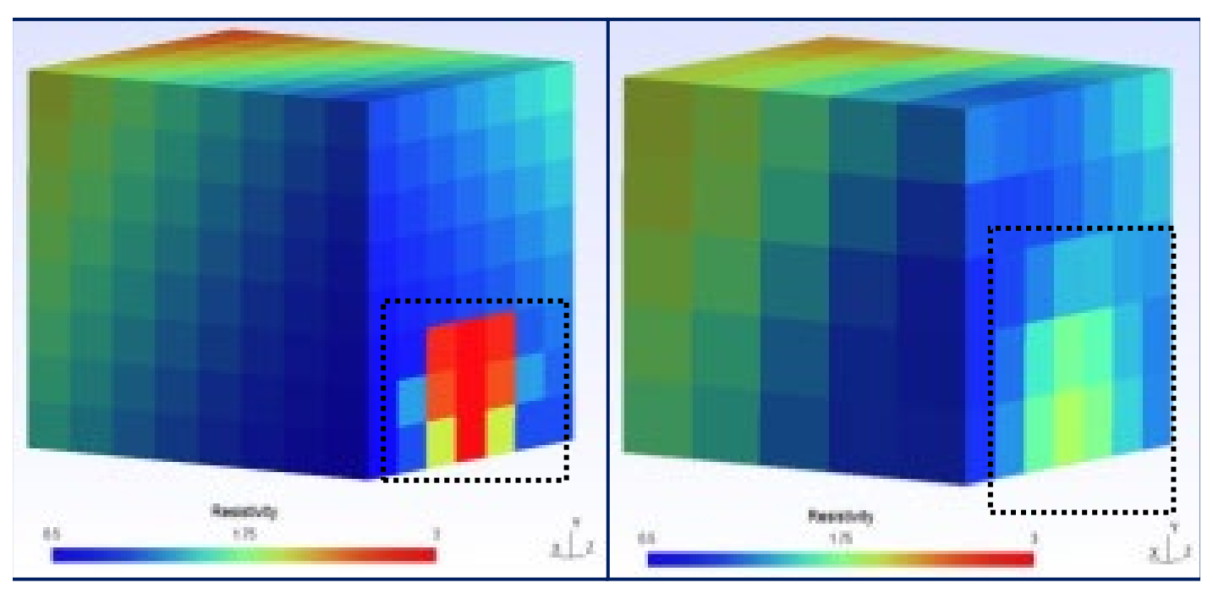

Initial resistivity map Identified resistivity map

- Good "fault" reproduction
- Fast convergence
- Good reproduction of the magnetic signature

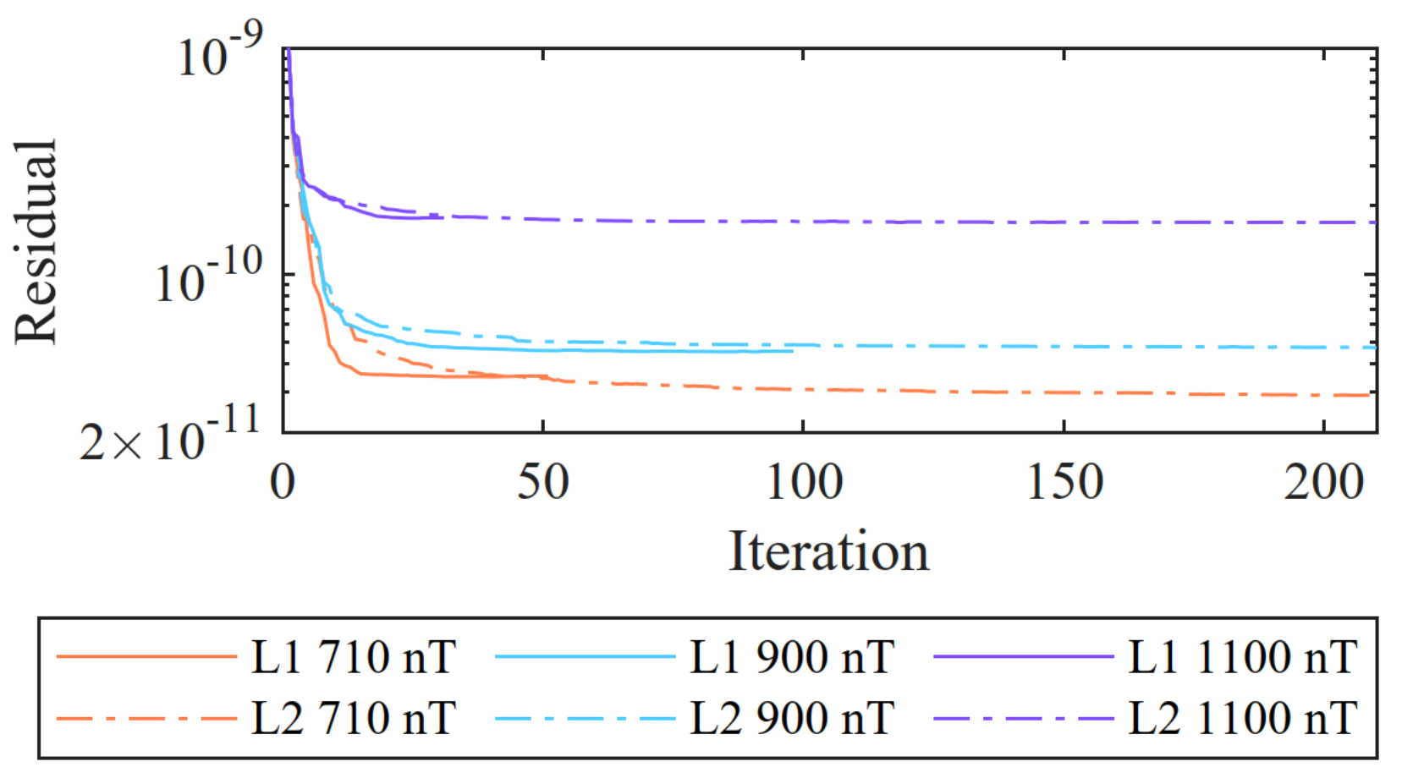

Optim. Convergence for different noise level and L1 and L2 regularization

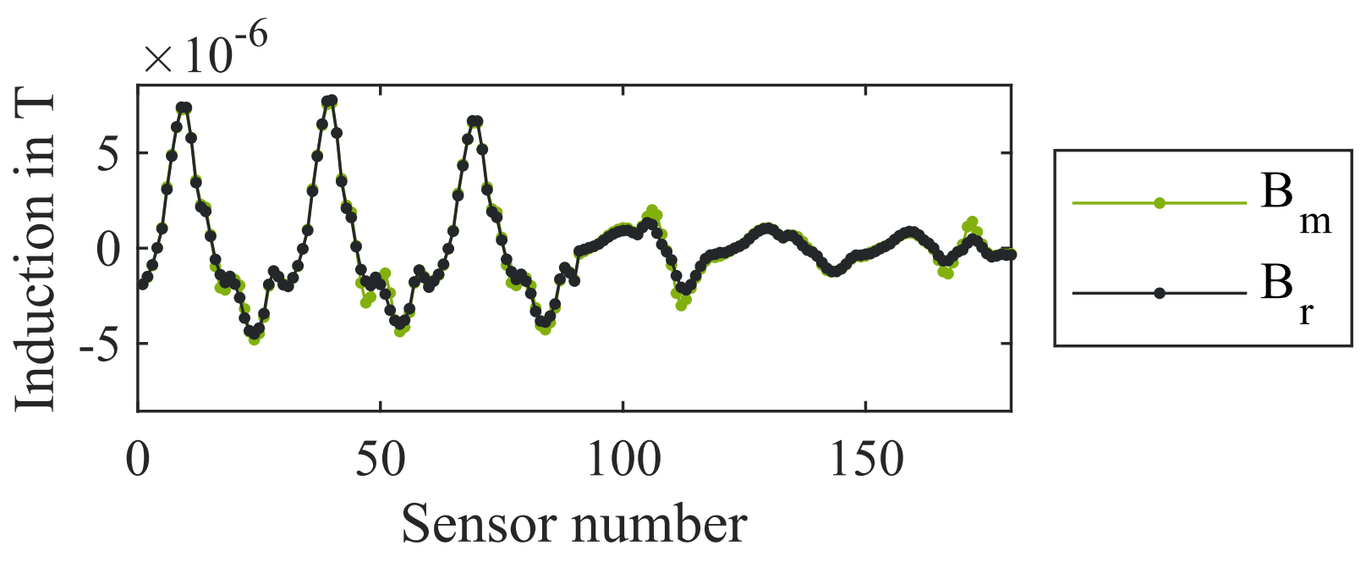

Magnetic field comparison between measured and reconstructed field on each sensor position

Real Measurement on a False Stack (only BPP and GDL)

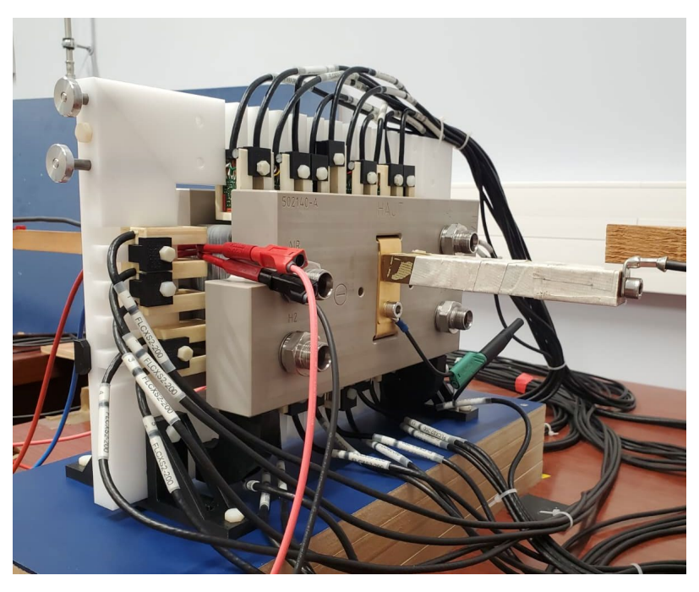

Procedure:

1. Local fault placed on membranes 20-21 inside the stack
2. Magnetic measurement
3. Data Treatment
4. Apply inverse method on data

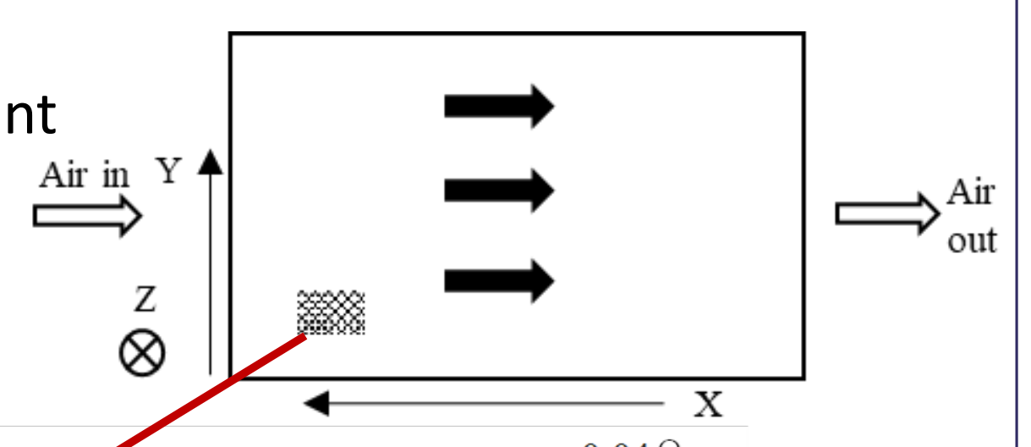

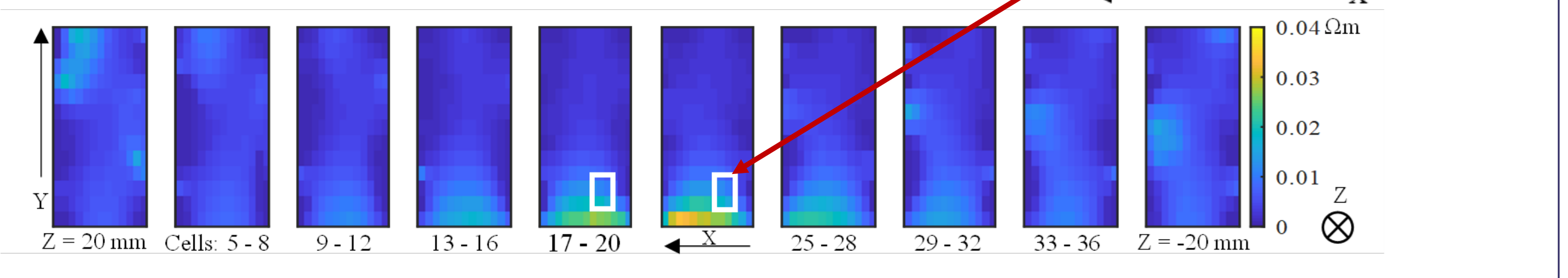

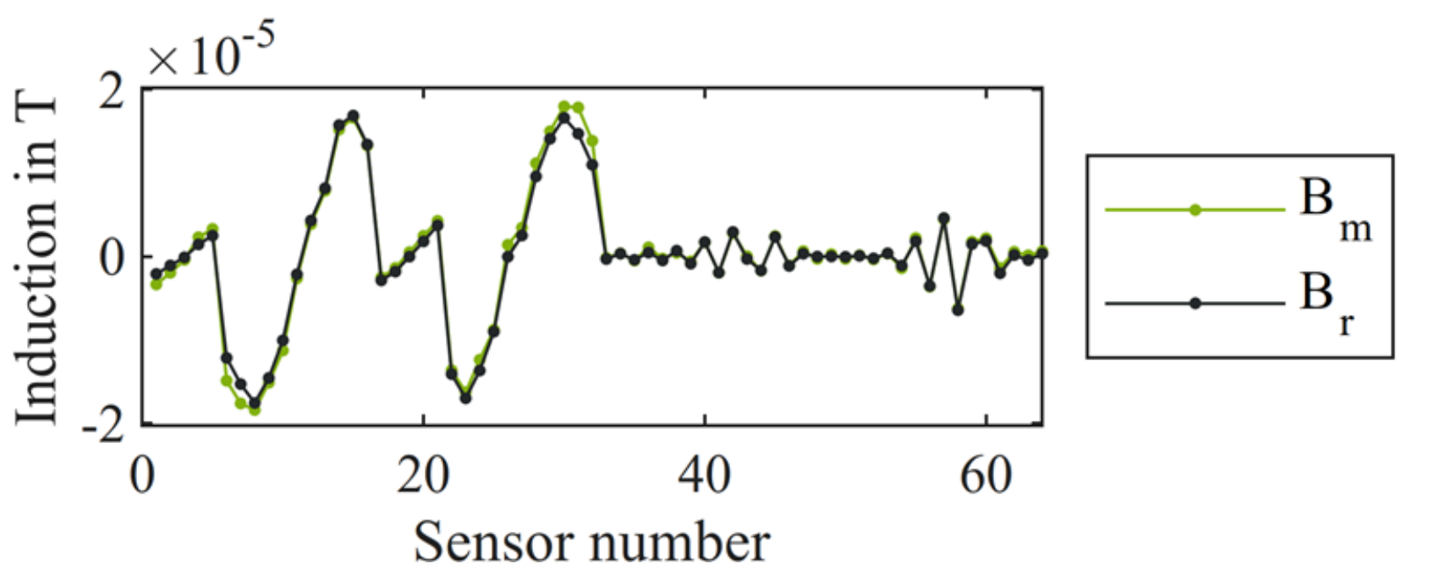

- A fault is successfully found ☺
- Fault is supposed to be in the two white rectangles 😐
- Fault is not at the correct position ☹
- A "propagation" can be seen along Cells 13 – 28

Key Takeaways

1. Requests only non-invasive measurements (U, I, B)
2. No prior knowledge needed
3. Successful reconstruction of resistivities from real measurement data
4. Converges within 20 steps
5. Permits a scalable mesh precision due to adjoint method (> 1000 variables)

References

[1] L. Ifrek, S. Rosini, G. Cauffet, O. Chadebec, L. Rouveyre, and Y. Bultel, "Fault detection for polymer electrolyte membrane fuel cell stack by external magnetic field," Electrochimica Acta, vol. 313, pp. 141–150, 2019.
[2] J. Cea, "Conception optimale ou identification de formes, calcul rapide de la dérivée directionnelle de la fonction coût," M2AN – Modélisation mathématique et analyse numérique, vol. 20, no. 3, pp. 371– 402, 1986.
[3] R. Fletcher, Practical methods of optimization, 2nd ed. Chichester; New York: Wiley, 2008.
[4] H. B. Curry, "The method of steepest descent for non-linear minimization problems," Quart. ppl. Math., vol. 2, no. 3, pp. 258–261, 1944, doi: 10.1090/qam/10667.
[5] P. C. Hansen, "Analysis of Discrete Ill-Posed Problems by Means of the L-Curve," SIAM Rev., vol. 34, no. 4, pp. 561–580, Dec. 1992, doi: 10.1137/1034115.

Parts of the present work are published in: Freisem, L., Chadebec, O., Cauffet, G., Rosini, S., & Bultel, Y. (2025). Gradient Descent-Based local equivalent resistivity identification for fuel cell diagnosis by magnetic tomography. *International Journal for Numerical Methods in Engineering*, *126*(21). https://doi.org/10.1002/nme.70168

L. FREISEM
R. RIASSE,
O. CHADEBEC,
G. CAUFFET,
Y. BULTEL,
F. MICOUD,
S. ROSINI

09/12/2025